Atherosclerosis 237 (2014) 739–747

Contents lists available at ScienceDirect

Atherosclerosis

journal homepage: www.elsevier.com/locate/atherosclerosis

Renin inhibition reduces atherosclerotic plaque neovessel formation and regresses advanced atherosclerotic plaques

Hongxian Wu [a], Xian Wu Cheng [a, b, d, *], Lina Hu [b], Chang-Ning Hao [a], Mutsuharu Hayashi [a], Kyosuke Takeshita [a], Mohammad Shoaib Hamrah [a], Guo-Ping Shi [c], Masafumi Kuzuya [b], Toyoaki Murohara [a, *]

[a] Department of Cardiology, Nagoya University Graduate School of Medicine, Nagoya, Japan
[b] Department of Community Healthcare & Geriatrics, Nagoya University Graduate School of Medicine, Nagoya, Japan
[c] Department of Medicine, Brigham and Women's Hospital, Harvard Medical School, United States
[d] Department of Cardiology, Yanbian University Hospital, Yanji, China

ARTICLE INFO

Article history:
Received 16 May 2014
Received in revised form
20 October 2014
Accepted 27 October 2014
Available online 30 October 2014

Keywords:
Aliskiren
Angiotensin II
Toll-like receptor 2
Cathepsin S
Atherosclerosis

ABSTRACT

Objective: The interaction between the renin-angiotensin system and toll-like receptors (TLRs) in the pathogenesis of advanced atherosclerotic plaques is not well understood. We studied the effects of the renin inhibitor aliskiren on the progression of advanced atherosclerotic plaque in apolipoprotein E-deficient ($ApoE^{-/-}$) mice with a special focus on plaque neovessel formation. **Methods and results**: Four-wk-old $ApoE^{-/-}$ mice were fed a high-fat diet for 8 wks, and the mice were randomly assigned to one of three groups and administered a vehicle, hydralazine, or aliskiren for an additional 12 wks. Aliskiren reduced the atherosclerotic plaque area and plaque neovessel density. It increased the plaque collagen and elastin contents, and reduced plasma angiotensin II levels and plaque macrophage infiltration and cathepsin S (CatS) protein. Aliskiren also decreased the levels of AT1R, gp91phox, TLR2, monocyte chemotactic protein-1, and CatS mRNAs in the aortic roots. Hydralazine had no beneficial vascular effects, although its administration resulted in the same degree of blood pressure reduction as aliskiren. CatS deficiency mimicked the aliskiren-mediated vasculoprotective effect in the $ApoE^{-/-}$ mice, but aliskiren showed no further benefits in $ApoE^{-/-}$ $CatS^{-/-}$ mice. *In vitro*, TLR2 silencing reduced CatS expression induced by angiotensin II. Moreover, aliskiren or the inhibition of CatS impaired the endothelial cell angiogenic action *in vitro* or/and *ex vivo*. **Conclusion**: Renin inhibition appears to inhibit advanced plaque neovessel formation in $ApoE^{-/-}$ mice and to decrease the vascular inflammatory action and extracellular matrix degradation, partly by reducing AT1R/TLR2-mediated CatS activation and activity, thus regressing advanced atherosclerosis.

1. Introduction

Increasing evidence shows that the renin-angiotensin system (RAS) play a pivotal role in the pathogenesis of atherosclerosis-based cardiovascular disease by stimulating a series of coordinated cellular and molecular events in atherosclerotic lesions [1]. Angiotensin II (Ang II) is a major bioactive component of the RAS and has been demonstrated to be a crucial mediator for atherosclerotic lesion development by inducing the production of reactive oxygen species and stimulating the expression of adhesion molecules and chemokines through the activation of the angiotensin II type 1 receptor (AT1R), thereby leading to endothelial dysfunction, the accumulation of inflammatory cells, lipid deposition, and the proliferation of vascular smooth muscle cells (SMCs) [1]. Aliskiren, a direct renin inhibitor which reduces the formation of angiotensin I from angiotensinogen, suppresses Ang II biosynthesis at the first step of the RAS [2]. A few experimental studies have reported the anti-atherosclerotic effects of aliskiren at the early stage of atherosclerosis [2,3]. However, the vasculoprotective action of aliskiren's renin inhibition on advanced atherosclerosis and its underlying mechanisms are not yet understood.

Recent advances in immunologic studies suggest that the toll-like receptor (TLR) system plays an important role in the pathogenesis of atherosclerosis [4]. Human atherosclerotic arteries

* Corresponding authors. Department of Cardiology, Nagoya University Graduate School of Medicine, 65 Tsuruma-cho, Showa-ku, Nagoya 466-8550, Japan.
E-mail addresses: xianwu@med.nagoya-u.ac.jp (X.W. Cheng), murohara@med.nagoya-u.ac.jp (T. Murohara).

http://dx.doi.org/10.1016/j.atherosclerosis.2014.10.098
0021-9150/

showed increased expressions of TLR-1, -2, and -4, compared to normal arteries [5]. The targeted deletion of TLR2 or TLR4 [6,7] or their downstream adaptor protein MyD88 [6] inhibited atherosclerotic lesion formation in apolipoprotein E-deficient ($ApoE^{-/-}$) mice. TLR2 has been shown to play an important role in monocyte activation and in stimulating the release of inflammatory chemokines and cytokines, which are crucial processes in the progression of atherogenesis [5]. Several lines of evidence indicate that RAS activation induces vascular inflammation through a TLRs-dependent signaling pathway [8]; however, the precise mechanisms of the RAS and the TLR signaling pathways in the progression of atherosclerosis remain unknown.

Neovascularization has been associated with advanced atherosclerotic plaque growth in diet-induced animal models [8,9]. Pharmacological inhibition of angiogenesis with endostatin and angiopoietin-2 overexpression has been reported to lead to a reduction of plaque neovascularization and growth [9]. Conversely, a number of experimental studies have shown that the stimulation of angiogenesis accelerates the progression of atherosclerotic plaque [10]. Angiogenic action stimulation has been closely linked to the Ang II/AT1R signaling pathway and protease activation (including matrix metalloproteinases (MMPs) and cysteinyl cathepsins) [8,11–13]. Cysteine protease cathepsins have also been implicated in the angiogenesis of pathophysiological conditions [14,15]. Several previous studies showed that cathepsin S (CatS) contributes to wound repair- or tumor growth-related angiogenesis [16,17]. However, the role of Ang II signaling in cathepsin activation-induced plaque neovessel formation and the mechanisms underlying the vasculoprotective action of the upstream inhibition of the RAS remain unclear, especially in atherogenesis at the advanced stage. To address these issues, we examined the effect of aliskiren-mediated RAS inhibition on the pathogenesis of advanced atherosclerosis in $ApoE^{-/-}$ mice, with a special focus on the plaque neovessel formation associated with TLR-dependent inflammation and cathepsin activation.

2. Materials and methods

2.1. Animals and treatment

All of the animal studies were conducted in accord with the animal care guidelines of the Nagoya University Graduate School of Medicine. Male $ApoE^{-/-}$ mice (C57BL/6 genetic background) were purchased from the Japan SLC (Hamamatsu, Japan). The animals were maintained in a 22 °C room with a 12-h light/dark cycle and received drinking water ad libitum. For the experiments, 4-wk-old male mice were fed a Western-type diet [18] containing 21.00% fat from lard and 0.15% cholesterol for 8 wks, and the mice were randomly assigned to one of three groups and administered vehicle (control, $n = 8$), hydralazine (25 mg mg/kg per day, in drinking water, Sigma–Aldrich; $n = 8$) or aliskiren (25 mg/kg per day via a subcutaneous [SC] mini-pump, Novartis, Basel, Switzerland; $n = 8$) for an additional 12 wks. In order to exclude the influence of mini-pump implantation, the control group and hydralazine group mice also underwent to a mini-pump implantation loaded with saline. Systolic blood pressure (BP) and heart rate (HR) were determined by using a tail-cuff pressure analysis system (Softron BP-98A, Tokyo) in conscious mice. Three reliable recordings were taken and used for the determination of systolic BP and HR.

In separate experiments, cathepsin S-deficient ($CatS^{-/-}$) mice (C57BL/6 background) were crossed with $ApoE^{-/-}$ mice (C57BL/6 background) to generate $ApoE^{-/-}$ $CatS^{-/-}$ mice. Male mice from both genetic backgrounds ($n = 6$ for each group) consumed an atherogenic Western-type diet [18] from 10 wks of age for 20 wks to allow the development of atherosclerotic lesions until sacrifice.

In another, separate experiment, aliskiren (25 mg/kg daily, by mini-pump; $n = 4$) or vehicle (saline; $n = 4$) was administered to $ApoE^{-/-}$ $CatS^{-/-}$ mice from 18 wks to 30 wks by supplementation of the Western-type diet (from the age of 10 wks).

2.2. Tissue collection and processing

Mice were anesthetized by an intraperitoneal injection of pentobarbital (50 mg/kg), and blood was collected from the cardiac apex for analysis. For histological and immunohistochemical staining, the hearts with aortic roots were dissected and immersed in fixative for 24 h (4 °C) and embedded in paraffin. For the biological analysis, aortic roots were stored in liquid nitrogen and RNAlater® solution (Life Technologies, Frederick, MD).

The cross-sections of the aortic root were analyzed according to the modified method of Matsumoto et al. [19] with a small modification. Each heart was cut in a plane between the lower tips of the right and left atria. The upper portion was embedded in paraffin. The aortic root was then sectioned (4 μm) serially at 5-μm intervals from the appearance of the aortic valve to the ascending aorta until the valve cusps were no longer visible. Five cross-sections in each aortic tissue were quantified for neointima and media, and the results for each mouse were averaged.

2.3. Histological and immunohistochemical staining and morphometry

Paraffin sections (4 μm) from the aortic roots were deparaffinized in xylene, rehydrated in decreasing alcohol solutions, and stained routinely with hematoxylin-eosin (H&E) staining, Elastica van Gieson staining (EVG) for elastin, and Picrosirius Red (PSR) staining for collagen as described [18]. We used the corresponding sections on separate slides for the immunohistochemical staining against macrophages (Mac-3; 1:100, BD Pharmingen, San Diego, CA) and CD31 (1:100, BD Pharmingen), CatS (M-19) (1:50, Santa Cruz Biotechnology, Santa Cruz, CA), α-smooth muscle cell actin (ASMA; 1:100, Sigma–Aldrich), and against monocyte chemotactic protein-1 (MCP-1; 1:500, Novus Biologicals, Littleton, CO). The positive areas for each stain were analyzed with BZ8000 analysis software (Keyence, Tokyo, Japan) or MetaMorph imaging analysis software (Molecular Devices, Sunnyvale, CA). Five cross-sections of vessels in each aorta were quantified and averaged for each animal. We set a threshold to automatically compute the positive areas for each stain and then computed the ratio of the positive area to the intimal area.

2.4. Human umbilical vein endothelial cells (HUVECs) culture and stimulations

HUVECs were purchased from Clonetics (San Diego, CA) and cultured in endothelial basal medium (EBM)-2 (Lonza, Walkersville, MD) plus 10% fetal bovine serum (FBS) and endothelial growth medium (EGM)-2 SingleQuots™ (Clonetics) in a humidified atmosphere of 5% CO_2 and 95% air. After being cultured in serum-free EBM-2 for 24 h, the HUVECs were used for the following experiments. The cells were treated with and without Ang II (100 nmol/L, Sigma–Aldrich) for 12 h and then subjected to quantitative real-time polymerase chain reaction (PCR) for the examination of TLR gene expression. To explore the mechanism of Ang II-induced CatS expression, we pretreated HUVECs with or without several inhibitors, including the AT1R antagonist olmesartan (10 μmol/L), the NADPH oxidase inhibitor apocynin (100 μmol/L), and the phosphatidylinositol-3-kinase (PI3K) inhibitor LY294002 (10 μmol/L, Calbiochem, EMD Chemicals, San Diego, CA). We performed five independent experiments in triplicate for each cell culture assay.

2.5. HUVECs small-interfering RNA transfection

Specific small-interfering RNA (siRNA) for TLR2 (siTLR2-I, F#55313524-001/2; siTLR2-II, F#55313524-003/4) and CatS (siCatS, #F52814467-001/2, #F52814467-003/4) and a negative control siRNA (F#5219292-009/010) were purchased from Sigma–Aldrich. siLamin A/C (D0010500105; Dharmacon, Brébières, France) was used as a positive control. siRNA was transfected into cells as described [20]. Briefly, 3.5×10^4 cells/well were grown on 6-well plates in EGM-2 without antibiotics until 30%–50% confluence. The siRNA solution was mixed with antibiotic-free Opti-MEM® I Reduced Serum Medium containing Lipofectamine™ RNAiMAX reagent (Invitrogen, Carlsbad, CA). The culture medium was removed and replaced with 2.5 mL of antibiotic-free EGM-2 medium, and then 500 μL of the transfection mix was added to each well (final siRNA concentration: 100 nmol/L for each control siRNA, 100 nmol/L for each siTLR2). Transfected cells were incubated with Ang II for 12 h and subjected to PCR assays.

2.6. Aortic ring culture for the angiogenesis assay

We performed an aortic ring assay for the quantification of angiogenesis as described [21]. Briefly, we inserted the rings from the aortas of $CatS^{+/+}$ and $CatS^{-/-}$ mice between two layers of type I collagen gel (BD Biosciences) and cultured in EBM-2 in the presence of vascular endothelial growth factor (VEGF) (20 ng/mL, Genzyme/Techne, Cambridge, MA) with or without aliskiren (10 μM), CatS specific inhibitor morpholinurea-leucine-homophenylalanine-vinylsulfone phenyl (LHVS), (5 nM, Arris Pharmaceutical, South San Francisco) or cathepsin non-specific inhibitor E64d (20 μM, Calbiochem, San Diego, CA) for 7 days. We performed a quantitative analysis of endothelial sprouts with the BZ8000 software. Endothelial cell sprouting density is expressed as a percentage of pixels per image occupied by vessels within a defined area.

2.7. HUVECs tubule formation assay

The tube formation assay was performed as described [20]. HUVECs (control and siRNA-transfected HUVECs with siTLR2 or siCatS, 2×10^4 cells/well) were seeded into 24-well tissue culture plates pre-coated with Matrigel (BD Biosciences) and cultured overnight in EBM-2 containing VEGF (50 ng/mL) to induce tube formation. Matrigel-induced tube formation was observed under a phase-contrast microscope (IIX 70, Olympus, Tokyo). We used the BZ8000 software to quantify the length of endothelial cell tubules in five fields (100×) in each well.

2.8. Quantitative real-time polymerase chain reaction

We isolated total RNA from the aortic roots and the lysates from HUVECs with the use of an RNeasy® Micro kit (Qiagen, Valencia, CA) and subjected it to reverse transcription. The resulting cDNA was subjected to a quantitative real-time PCR analysis with the use of a Bio-Rad CFX96™ Real-Time PCR Detection System and Power SYBR® Green PCR Master Mix (Applied Biosystems, Foster City, CA) or Applied Biosystems Prism 7500HT sequence detection system using TaqMan gene expression assays according to the manufacturer's specifications (Applied Biosystems, Foster City, CA). We calculated the changes in gene expression by the $2^{-\Delta\Delta Ct}$ method and normalized the values to the levels of glyceraldehyde 3-phosphate dehydrogenase (GAPDH). All samples were analyzed in triplicate. TaqMan probes and primers are as follows: TNF-α: Mm00443258_m1; iNOS: Mm00440502_m1; Arginase-1: Mm00475988_m1; CD206: Mm00485148_m1; FIZZ1: Mm00445109_m1; 18S ribosomal RNA: 4319413E. Primers for SYBR® Green assay are shown in Online supplementary Table 1.

2.9. Western blotting analysis

Total extracted protein from aortic roots and HUVECs was separated with 10% SDS-PAGE and then transferred to a polyvinylidene difluoride membrane (Amersham Pharmacia Biotech, Buckinghamshire, UK). Nonspecific binding was blocked with 5% skim milk/Tris-buffered saline with Tween for 1 h at room temperature and then incubated with primary antibodies against TLR2 (H-175) and CatS (all from Santa Cruz, diluted 1:1000) at 4 °C overnight. β-actin was loaded as control. The band intensity was analyzed by densitometry using Image J software.

2.10. Biochemical analysis

We examined the plasma renin activity (PRA) using a radioimmunoassay of generated Ang I (SRL renin kit, TFB Co., Tokyo). The plasma Ang II concentrations were measured by a radioimmunoassay (human NEX-105 [125]I-Try4-Angiotensin II, Perkin Elmer Life and Analytical Sciences, Boston, MA). The plasma total cholesterol and triglyceride concentrations were determined with enzymatic assay kits (Wako Pure Chemical Industries, Osaka, Japan). The plasma glucose concentrations were measured using an automatic glucometer (One Touch Ultra; LifeScan, Milpitas, CA). All assays were performed in triplicate.

2.11. Statistical analysis

All measurements were conducted by two observers blinded to the treatment of the mice. Data are expressed as means ± standard error of the mean (SEM). Student's *t*-test (for comparisons between two groups) and a one-way analysis of variance (ANOVA; for comparisons of three or more groups) followed by the Bonferroni post-hoc test were used for the statistical analyses. The HR and BP data were subjected to a two-way repeated-measures ANOVA and Bonferroni post hoc tests. SPSS software ver. 17.0 (SPSS, Chicago, IL) was used. *P*-values <0.05 were considered significant.

3. Results

3.1. Effect of aliskiren on systolic BP, HR, plasma lipid profiles, and the PRA and plasma Ang II levels

After 12 wks of treatment, aliskiren reduced the systolic BP in the mice, but had no effect on their body weight (BW) or HR compared to the corresponding values of the control group (Online supplementary Table 2). Aliskiren also had no significant effect on plasma total cholesterol, triglyceride, or glucose (Online supplementary Table 2). However, the aliskiren-treated mice

Table 1
Histological characterization of atherosclerotic lesions in the aortic roots of control, aliskiren and hydralazine-treated mice.

Parameters	Control	Hydralazine	Aliskiren
	$n = 8$	$n = 8$	$n = 8$
Intima ($\times 10^3/\mu m^2$)	612 ± 19	588 ± 37	287 ± 30*
Media ($\times 10^3/\mu m^2$)	306 ± 17	319 ± 25	300 ± 28
Intima/media ratio	2.10 ± 0.14	1.95 ± 0.14	0.96 ± 0.04*

The ratio of intima to media was calculated as the ratio of the intimal area to the media area in lesional cross-sections of the heart aortic root of control, aliskiren and hydralazine-treated groups. All of the results are presented as mean ± SEM. *$P < 0.01$ vs corresponding control groups.

showed significant decreases in PRA and plasma Ang II. Except lowering systolic BP, hydralazine treatment showed no effect on these parameters as compared to the control group (Online supplementary Table 2).

3.2. Aliskiren reduced the extent of atherosclerotic lesions and neovessel plaque density and changed the plaque composition

The H&E staining showed that aliskiren treatment significantly reduced the area of the neointima in the aortic lesional regions as well as the ratio of the intima area to the media area compared to that of the controls ($P < 0.01$; Table 1). Immunohistochemistry revealed that aliskiren reduced the neovessel density of the atherosclerotic plaques in the aortic roots (total neovessel numbers: 7.9 ± 1.2 vs. 18.0 ± 1.7 mm^2 in the aliskiren and control groups, respectively; $P < 0.01$; Fig. 1). In contrast, hydralazine had no effects on these parameters (Table 1, Fig. 1A and B).

As shown in Fig. 1A and C, aliskiren significantly increased the interstitial collagen content of the neointima (45.0 ± 1.8% vs. 34.8 ± 2.2% in the aliskiren and control groups, respectively; $P < 0.01$) as determined by PSR staining. In addition, the elastin level of the neointimas determined by EVG staining remained significantly higher in the aliskiren-treated mice compared to the control mice (12.5 ± 0.7% vs. 7.8 ± 1.0%, respectively; $P < 0.01$; Fig. 1A and D). Hydralazine had no effect on the plaque matrix components.

3.3. Aliskiren decreased the vascular inflammatory action and CatS expression in the aortic roots

As shown in Fig. 2A and B, the accumulation of macrophages (Mac-3) was significantly suppressed by aliskiren treatment. Immunostaining revealed that aliskiren attenuated the levels of MCP-1 protein (Fig. 2A and C). As shown in Fig. 2A and D, aliskiren markedly decreased the CatS protein expression in the atherosclerotic plaques of the aortic roots, whereas hydralazine treatment showed none of these beneficial effects compared to the control group. In addition, aliskiren had no effect on the accumulation of SMCs in the atherosclerotic plaques of the aortic roots (Fig. 2A and E). Concomitantly, quantitative PCR revealed that aliskiren attenuated the mRNA levels of AT1R, gp91phox, TLR2, MCP-1, VCAM-1, and CatS in the aortic roots compared to the control group (Fig. 3A–F).

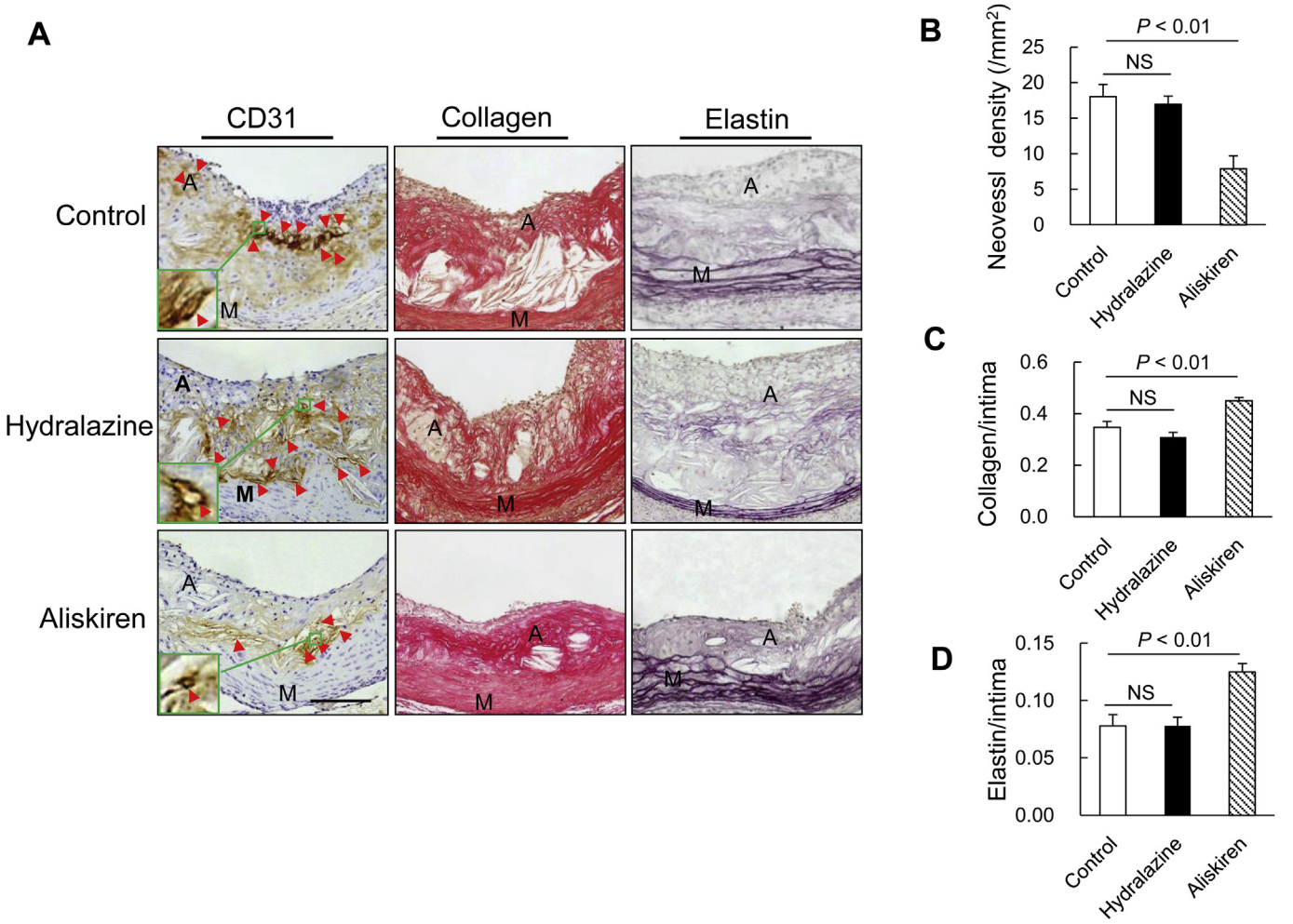

Fig. 1. Detection of neovessel density and collagen and elastin content of advanced atherosclerotic lesions in the aortic roots of apolipoprotein E-deficient ($ApoE^{-/-}$) mice treated with vehicle (control, $n = 8$), aliskiren (25 mg/kg·d, $n = 8$), or hydralazine (25 mg/kg·d, $n = 8$) for 12 wks. A: Representative images used to assess neovessel density (CD31 immunostaining) and the content of collagen (PSR staining) and elastin (EVG staining). B–D: Quantitative data for neovessel density (B, $n = 7$), collagen (C, $n = 8$) and elastin (D, $n = 8$) positive areas in atherosclerotic lesion intimas. The neovessel density data are expressed as total numbers of neomicrovessels divided by the plaque area (in mm^2). A, atheroma; M, media. Scale bars: 100 μm.

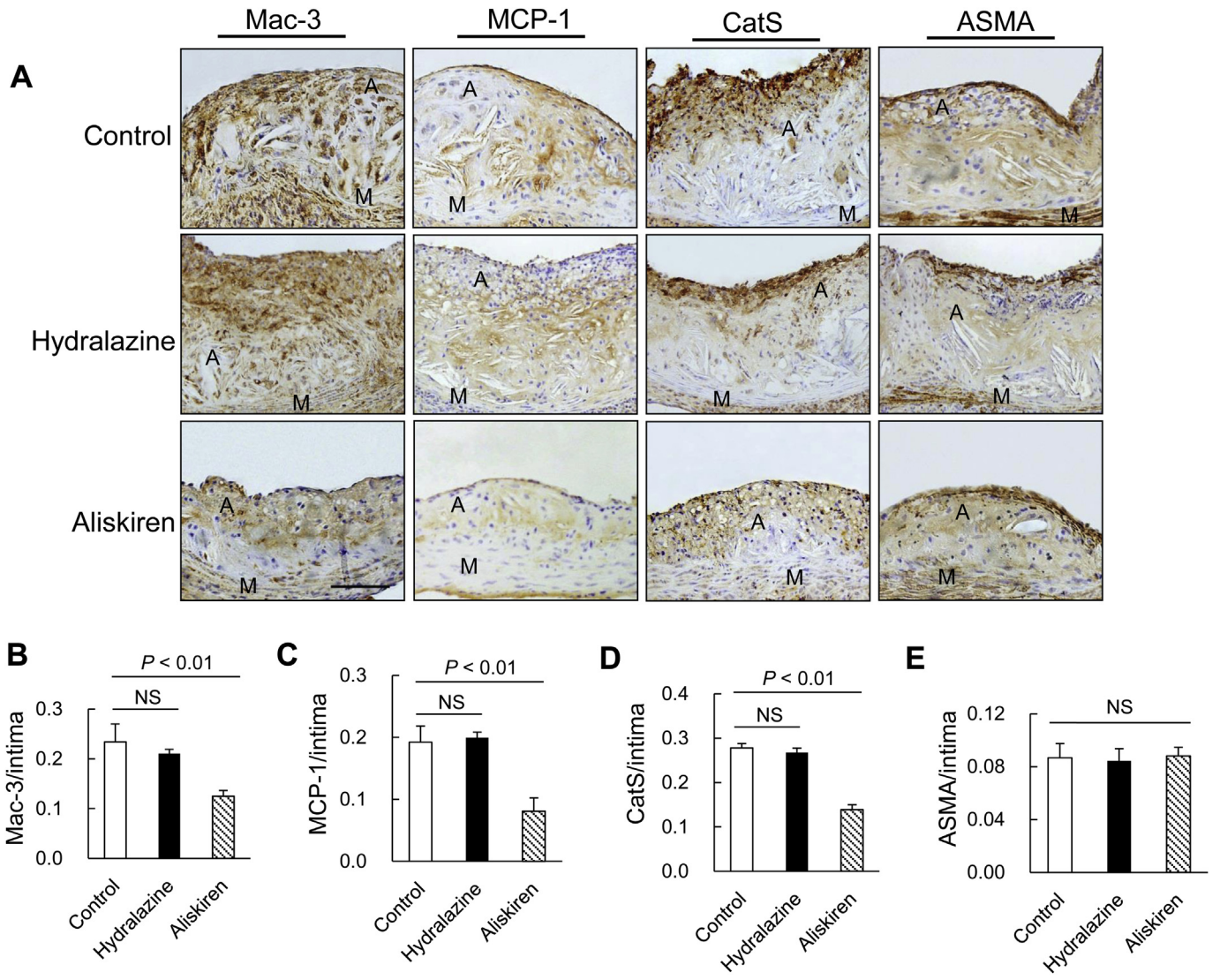

Fig. 2. Histological characterization of advanced atherosclerotic lesions in aortic roots of the control, aliskiren, and hydralazine groups ($n = 8$, each group). A: Representative immunostaining images used to assess the content of macrophages (Mac-3) and MCP-1, CatS proteins, and α-smooth muscle cell actin (ASMA) SMCs. B–E: The positive areas in the atherosclerotic lesion intimas for Mac-3 (B), MCP-1 (C), CatS (D), and ASMA (E) were quantified for each section. Results are expressed as the ratio (percentage) of the positively stained area to the neointimal area. A, atheroma; M, media. Scale bars: 100 μm.

3.4. Effect of aliskiren on macrophage M2 polarization in the aortic roots

To determine the effect of aliskiren on macrophage polarization in the atherosclerotic lesions, we evaluated M1-and M2-related marker gene expressions in the aortic roots. The quantitative real-time PCR analysis revealed that aliskiren reduced the expression of activated M2 (arginase-1, CD206, FIZZ1) markers and had no effect on the ratio of arginase-1 to iNOS as compared with the control group (Online supplementary Fig. 1), indicating that aliskiren could not enhance macrophage M2 polarization.

3.5. CatS deficiency reduced the intimal neovessel density and plaque growth

Compared to the control mice, the CatS$^{-/-}$ mice showed reduced plaque growth and intimal neovessel density in the aortic roots, as determined by immunohistochemical staining against CD31 (Online supplementary Fig. 2A–C) [22]. We also observed a lower level of macrophage accumulation (Online supplementary Fig. 2A and D) and increased contents of collagen and elastin in the atheroma plaques of the aortic roots in the ApoE$^{-/-}$ CatS$^{-/-}$ mice (Online supplementary Fig. 3A–C). Furthermore, CatS deficiency reduced the levels of TLR2 gene expression in the aortic roots of the ApoE$^{-/-}$ mice (Online supplementary Fig. 3D). Aliskiren treatment had no significant effect on the atherosclerotic lesion growth or the neovessel formation of aortic roots in the ApoE$^{-/-}$ CatS$^{-/-}$ mice ($P > 0.05$; Online supplementary Fig. 4).

In addition, quantitative real-time PCR revealed that although CatS ablation reduced activated M1 markers (TNF-α and iNOS), it showed no effects on activated M2 markers (arginase-1, CD206, FIZZ1) as compared with ApoE$^{-/-}$ CatS$^{+/+}$ mice (Online supplementary Fig. 5), indicating that CatS deficiency might not affect M2 genetic program in atherosclerosis.

3.6. Ang II regulates CatS gene expression through TLR2 signaling pathway

As shown in Fig. 4A and B, Ang II increased the TLR2 and CatS mRNA expressions in the cultured HUVECs. As anticipated, siTLR2

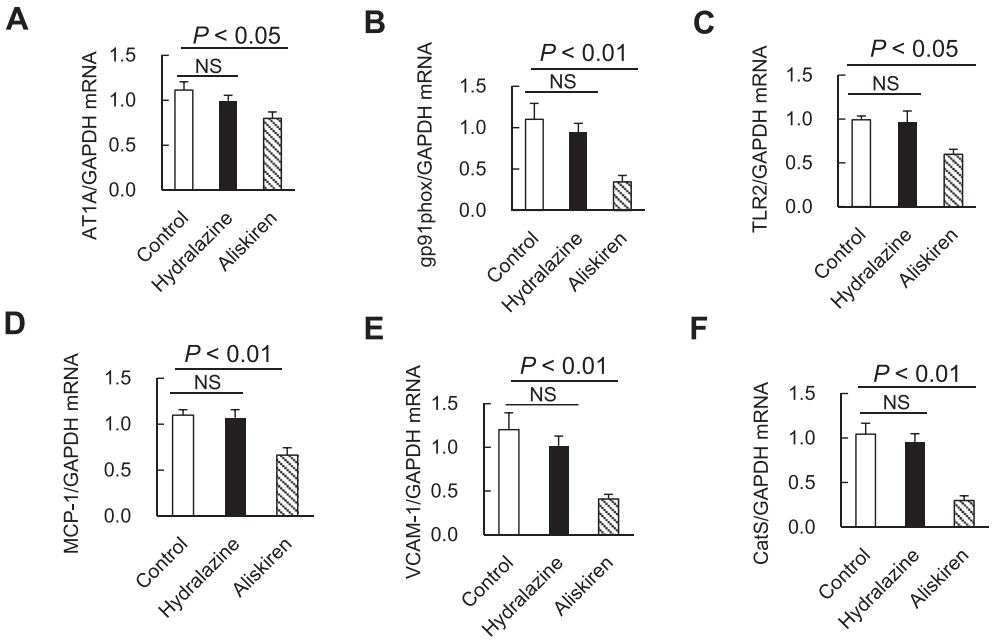

Fig. 3. Aliskiren decreased the vascular inflammatory action and CatS expression in the aortic roots of ApoE$^{-/-}$ mice. A–F: A real-time PCR analysis was used to determine the mRNA levels of AT1R, gp91phox, TLR2, MCP-1, VCAM-1, and CatS of the aortic roots of the control, aliskiren, and hydralazine groups ($n = 8$ each). Values are mean ± SEM.

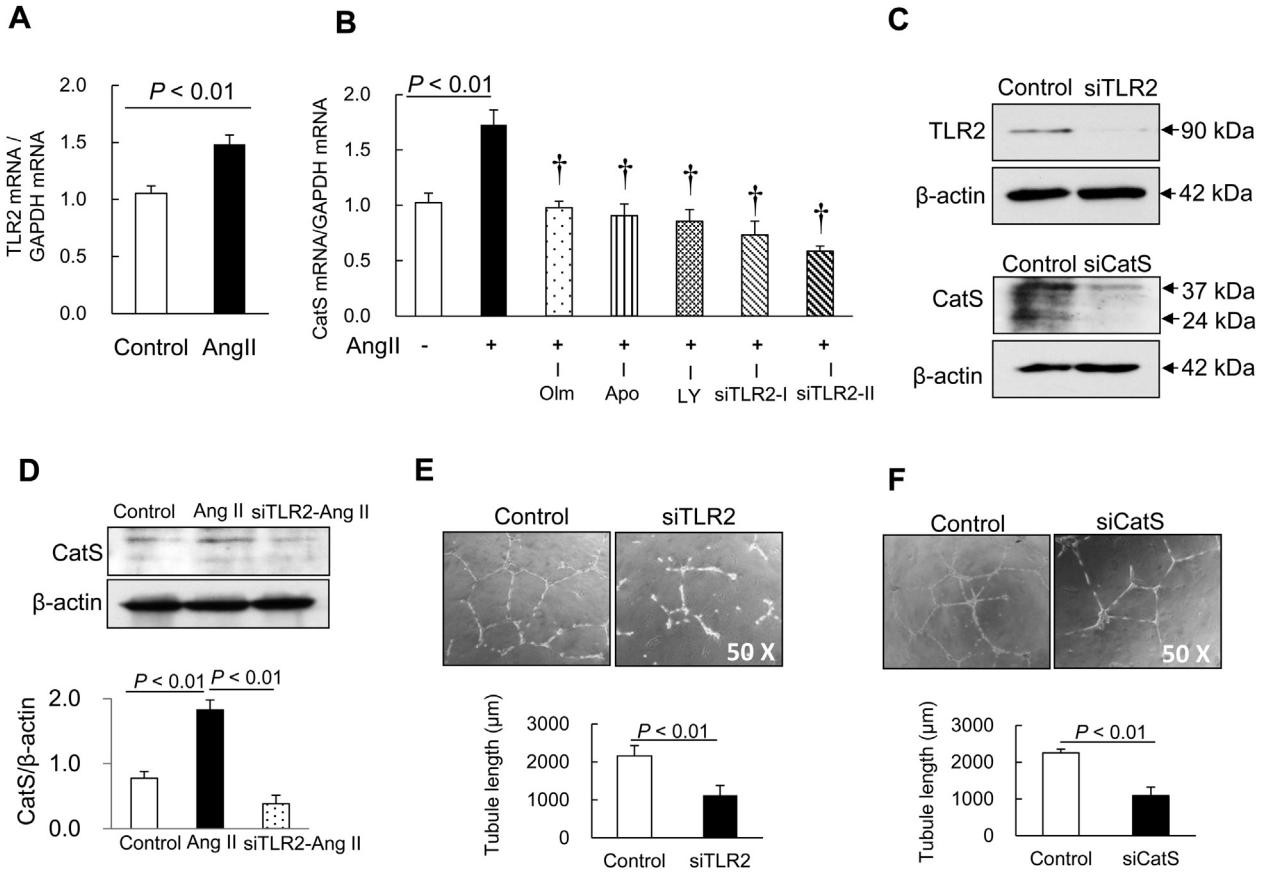

Fig. 4. Regulation of TLR2 and CatS gene expression in HUVECs. A: Real-time PCR analysis to detect TLR2 mRNA levels in HUVECs stimulated with or without Ang II (100 nmol/L) for 12 h ($n = 5$). B: After pretreatment with or without olmesartan (Olm, 10 μmol/L), apocynin (Apo, 100 μmol/L) or LY294002 (LY, 10 μmol/L) for 30 min or transfection with siTLR2-I or siTLR2-II (100 nmol/L), respectively, for 48 h, the HUVECs were cultured in the presence or absence of Ang II for 12 h and then were subjected to CatS gene assay ($n = 5$, each group). $^{\dagger}P < 0.01$ vs. Ang II (+). C: Representative images show siTLR2 and siCatS reduces its targeted protein expression proteins in HUVECs transfected with non-siRNA, siTLR2 or siCatS, respectively, for 48 h ($n = 4$). D: Representative images and combined quantitative data for the siCatS-mediated suppression on CatS expression induced by Ang II in HUVECs. E, F: Representative images and quantitative data for tubulogenesis ($n = 6$). Values are mean ± SEM.

and siCatS suppressed the levels of TLR2 or CatS protein, respectively (Fig. 4C). By comparison, siTLR2 also inhibited CatS protein expression induced by Ang II (Fig. 4D). We next investigated the mechanisms underlying the Ang II-mediated CatS expression in HUVECs by examining the effect of several inhibitors on intracellular signaling pathways. Pretreatment with the AT1R antagonist olmesartan, the NADPH oxidase inhibitor apocynin, and the phosphatidylinositol 3-kinase inhibitor LY294002 reduced the expressions of CatS mRNA stimulated by Ang II in HUVECs (Fig. 4B). Similar to the Western blot assay, both siTLR2-I and siTLR2-II significantly reduced CatS gene expression (Fig. 4B). By comparison, the non-target control siRNA had no effect on the TLR2 gene expression induced by Ang II (data not shown).

3.7. *Effect of aliskiren or TLR2 and CatS ablation on the angiogenic action*

Both siTLR2 and siCatS inhibited the VEGF-induced HUVEC tubulogenic action (Fig. 4E and F). The *ex vivo* aortic ring culture assays showed that CatS deficiency impaired VEGF-mediated aorta-derived microvessel outgrowth (Fig. 5A and B). Furthermore, we observed that aliskiren as well as cathepsin inhibitors (a specific CatS inhibitor LHVS and non-specific cathepsin inhibitor E64*d*) suppressed VEGF-induced angiogenic response of the aorta from the $CatS^{+/+}$ mice (Fig. 5C and D).

4. Discussion

Previous experimental studies showed that direct renin inhibition with aliskiren inhibits the development of early atherosclerosis [2,3]. Here we have demonstrated that aliskiren has a vasculoprotective effect on advanced atherosclerosis. Our study showed that Ang II inhibition by renin inhibition with aliskiren not only lessened the progression of atherosclerotic lesions but also changed the composition of the vascular wall such that it contained more

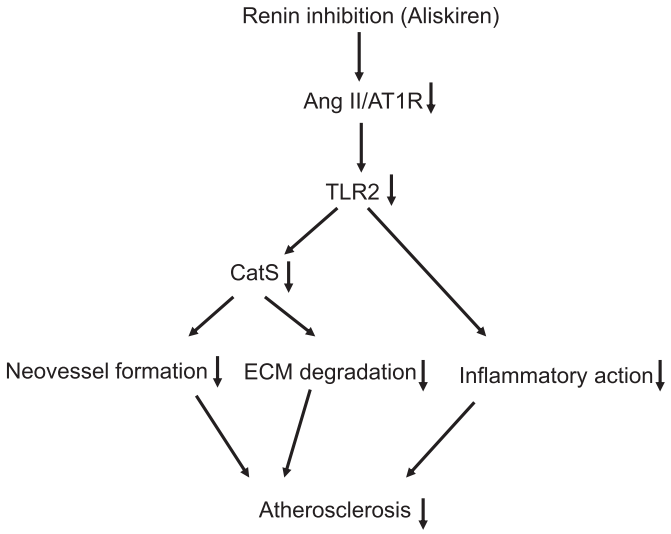

Fig. 6. The proposed mechanism of aliskiren-mediated regression of advanced atherosclerotic plaques in the $ApoE^{-/-}$ mouse model. Ang II, angiotensin II; AT1R, angiotensin II type 1 receptor; TLR2, toll-like receptor 2; CatS, cathepsin S; ECM, extracellular matrix.

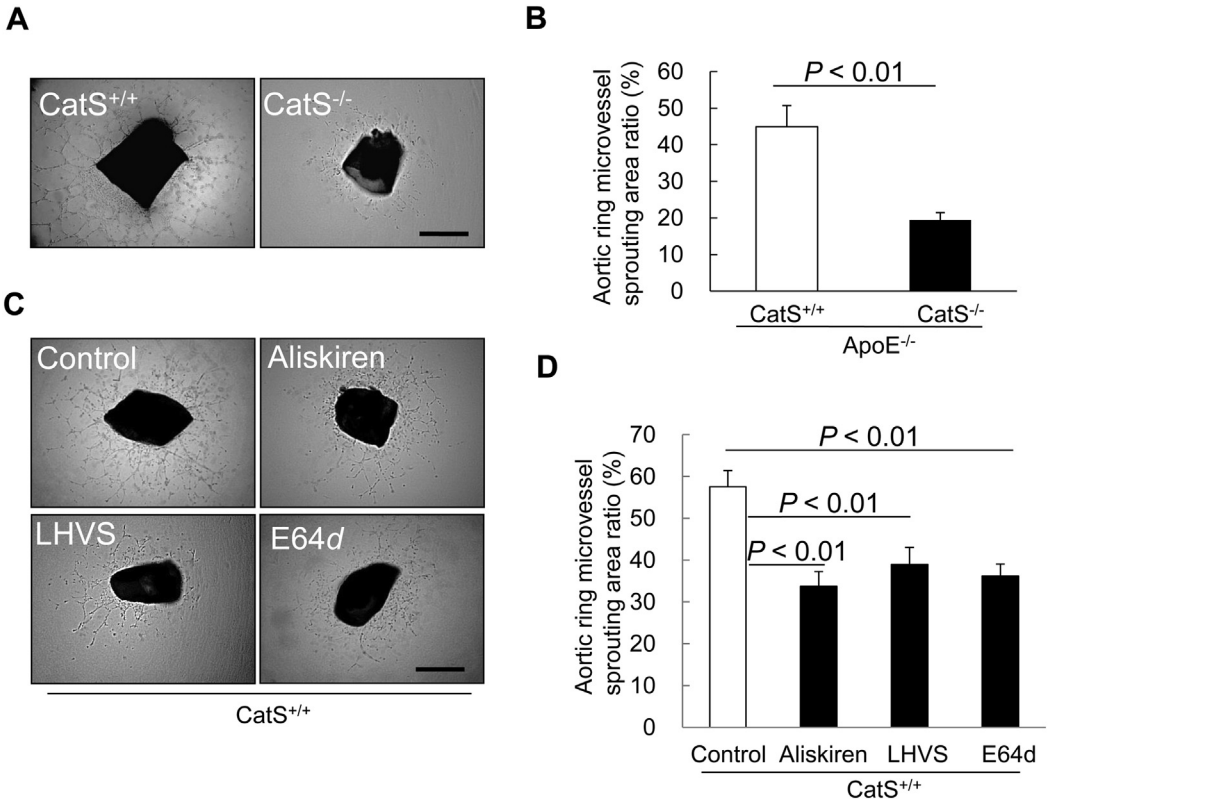

Fig. 5. Aliskiren reduced the angiogenic activity of aortic explants. Aortic rings were reversed and cultured in serum-free EBM-2 medium with VEGF (20 ng/mL) for 7 days. A, B: Representative images and combined quantitative data for tubulogenesis in the aortas of $CatS^{+/+}$ and $CatS^{-/-}$ mice ($n = 6$). Scale bars: 1 mm. C, D: Aortic rings from $CatS^{+/+}$ mice were induced with 20 ng/mL VEGF in the presence or absence of aliskiren (10 μM) and Cat inhibitors (LHVS, 5 nM; E64*d*, 20 μM). Representative images (C) and quantitative data (D) for aortic ring microvessel sprouting area. Scale bars: 50 μm.

extracellular matrix protein (collagen and elastin), changes that predict greater stability of the atherosclerotic plaque. Renin inhibition also reduced the diet-induced intimal neovascularization in atherosclerotic plaques, which was accompanied by a reduced accumulation of macrophages and reduced expression of CatS associated with the reduction in TLR2 gene expression. More notably, we showed that CatS deficiency lessened diet-induced atherosclerotic plaque neovessel formation and growth, as well as the levels of TLR2 mRNA and macrophage infiltration in ApoE$^{-/-}$ mice. Our *in vitro* experiment also demonstrated Ang II induced CatS gene expression via the TLR2-mediated signaling pathway. Our proposal regarding the mechanisms underlying the aliskiren-mediated renin inhibition in the reduction of atherosclerotic plaque neovessel formation and the improvement of established atherosclerotic plaques is represented schematically in Fig. 6.

Ang II is suggested to be a key player in the pathogenesis of atherosclerosis, by inducing the production of reactive oxygen species and stimulating the expression of adhesion molecules, chemokines, and proteases through activation of the AT1R [1,23]. Previous studies indicated that Ang II regulates TLRs expression [24,25], and the engagement of TLRs on the cell surface by specific ligands regulates monocyte/macrophage activation and leads to an increase in the expression of proinflammatory mediators such as MCP-1 [26]. A recent study showed that TLR2 signaling through MyD88 plays a predominant role in inflammation and matrix degradation in human atherosclerosis [27]. Here, we found that the renin inhibitor aliskiren lessened the progression of atherosclerotic lesions and resulted in reductions in plasma Ang II and in the mRNA levels of AT1R, gp91phox, TLR2, MCP-1, and VCAM-1 in atherosclerotic lesions. Thus, renin inhibition appears to reduce atherosclerotic lesions in ApoE$^{-/-}$ mice through its ability to attenuate Ang II-AT1R/TLR2-mediated inflammatory chemokine and oxidative stress production. It should be noted that hydralazine reduced the blood pressure of the mice to the same extent as aliskiren but had no vascular benefits compared to aliskiren. Moreover, the daily administration of aliskiren at the dose used in this study had no significant effect on the animals' lipid profiles. In addition, we have shown that aliskiren reduced M2 marker gene expressions and had no effect on the ratio of iNOS to arginase-1 genes. These results suggest that aliskiren-mediated advanced atherosclerotic plaque regression is not attributable to blood pressure reduction, lipid reduction, or M1/M2 polarization but rather to the pleiotropic effects of aliskiren.

Cysteine protease cathepsins have been implicated in a number of pathologies associated with extracellular matrix (ECM) breakdown [14,28]. Here we found that Ang II inhibition with aliskiren reduced ECM degradation as well as the mRNA and protein levels of CatS in aortic roots. Several previous studies showed that CatS contributes to angiogenesis in the process of wound repair or tumor growth [16,17]. Here, *in vitro*, we observed that siTLR2 and siCatS impaired the cultured HUVEC tubulogenic action. Our results further confirm that CatS participates in angiogenesis by the *ex vivo* aortic ring culture assays. Recent observations indicate that plaque angiogenesis contributes to plaque instability and the rupture of advanced atherosclerotic lesions in human aortas [29]. Here, we found that aliskiren treatment also reduced plaque vessel formation. Combined with the previous findings, our results indicate that the ability of renin inhibition to decrease CatS gene expression is likely to have contributed to the observed reduction in neovessel density and the stabilization of advanced atherosclerotic lesions in ApoE$^{-/-}$ mice. This notion is further supported by our current observations that the atherosclerotic plaque neovessel density and lesions were reduced in the ApoE$^{-/-}$ CatS$^{-/-}$ mice, and renin inhibition had no additional benefit on the atherosclerotic lesion formation in the ApoE$^{-/-}$ CatS$^{-/-}$ mice. Collectively, these findings suggest that the attenuation of neovascularization and ECM remodeling by renin inhibition via the inhibition of CatS expression represents a common mechanism for the reduction of diet-induced advanced atherosclerotic plaque growth and stability.

Previous studies showed that Ang II regulates the expression of TLRs in vascular smooth muscle cells and dendritic cells [24,25]. A single study demonstrated that TLR activation induces cysteine protease CatK expression in cultured macrophages [30]. The present data show that angiotensin inhibition with a renin inhibitor reduces the mRNA levels of CatS and TLR2 in aortic tissues. Consistent with this, we have also confirmed *in vitro* for the first time that pretreatment with the AT1R antagonist olmesartan reduces the expression of Ang II-induced TLR2 and CatS mRNA. Increasing evidence highlighted the importance of protease induction through the activation of TLRs [8]. Here, we have further demonstrated that siRNA targeting TLR2 reduced the CatS gene expression induced by Ang II in HUVECs. Taken together, these findings suggest that there might be crosstalk between the Ang II/AT1R and TLR2 signaling pathways in vascular cells and that the renin inhibition-mediated reduction of TLR2 expression might be involved, at least in part, in the inhibitory effect of renin inhibition on CatS gene expression. In 2009, Sun and colleagues reported that several signaling pathways were involved in TLR-mediated CatK expression in cultured macrophages [30]. Here we found that the CatS expression induced by Ang II in HUVECs was inhibited by the PI3K inhibitor LY294002, indicating that the PI3K/Akt signaling pathway is involved in the Ang II-mediated regulation of CatS expression.

In summary, our study provides new insights into the mechanisms of renin inhibition in the improvement of advanced atherosclerosis. Renin inhibition appears to inhibit intimal neovascularization in ApoE$^{-/-}$ mice and to decrease the vascular inflammatory action and extracellular matrix degradation, partly by reducing the AT1R/TLR2-mediated CatS activation, thus regressing advanced atherosclerosis.

Sources of funding

This work was supported by the Hori Sciences and Arts Foundation (no. 26-007737 to H.W.), and partly by grants from the Ministry of Education, Culture, Sports, Science, and Technology of Japan (no. 24659385 to X.W.C.; no. 20249045 to T.M.).

Disclosures

The authors have no conflict of interest to declare.

Appendix A. Supplementary data

Supplementary data related to this article can be found at http://dx.doi.org/10.1016/j.atherosclerosis.2014.10.098.

References

[1] A. Daugherty, L. Cassis, Angiotensin II-mediated development of vascular diseases, Trends Cardiovasc. Med. 14 (2004) 117–120.
[2] H. Lu, D.L. Rateri, D.L. Feldman, R.J. Charnigo, A. Fukamizu, J.J. Ishida, et al., Renin inhibition reduces hypercholesterolemia-induced atherosclerosis in mice, J. Clin. Investig. 118 (2008) 984–993.
[3] T. Imanishi, H. Tsujioka, H. Ikejima, A. Kuroi, S. Takarada, H. Kitabata, et al., Renin inhibitor aliskiren improves impaired nitric oxide bioavailability and protects against atherosclerotic changes, Hypertension 52 (2008) 563–572.
[4] C. Weber, H. Noels, Atherosclerosis: current pathogenesis and therapeutic options, Nat. Med. 17 (2011) 1410–1422.
[5] K. Edfeldt, J. Swedenborg, G.K. Hansson, Z.Q. Yan, Expression of toll-like receptors in human atherosclerotic lesions – a possible pathway for plaque activation, Circulation 105 (2002) 1158–1161.

[6] K.S. Michelsen, M.H. Wong, P.K. Shah, W.X. Zhang, J.A. Yano, T.M. Doherty, et al., Lack of toll-like receptor 4 or myeloid differentiation factor 88 reduces atherosclerosis and alters plaque phenotype in mice deficient in apolipoprotein E, Proc. Natl. Acad. Sci. U. S. A. 101 (2004) 10679–10684.
[7] X. Liu, T. Ukai, H. Yurnoto, M. Davey, S. Goswami, F.C. Gibson, et al., Toll-like receptor 2 plays a critical role in the progression of atherosclerosis that is independent of dietary lipids, Atherosclerosis 196 (2008) 146–154.
[8] X.W. Cheng, H.Z. Song, T. Sasaki, L.N. Hu, A. Inoue, Y.K. Bando, et al., Angiotensin type 1 receptor blocker reduces intimal neovascularization and plaque growth in apolipoprotein e-deficient mice, Hypertension 57 (2011), 981–U238.
[9] K.S. Moulton, E. Heller, M.A. Konerding, E. Flynn, W. Palinski, J. Folkman, Angiogenesis inhibitors endostatin or TNP-470 reduce intimal neovascularization and plaque growth in apolipoprotein E-deficient mice, Circulation 99 (1999) 1726–1732.
[10] F.L. Celletti, J.M. Waugh, P.G. Amabile, A. Brendolan, P.R. Hilfiker, M.D. Dake, Vascular endothelial growth factor enhances atherosclerotic plaque progression, Nat. Med. 7 (2001) 425–429.
[11] X.W. Cheng, Z. Huang, M. Kuzuya, K. Okumura, T. Murohara, Cysteine protease cathepsins in atherosclerosis-based vascular disease and its complications, Hypertension 58 (2011) 978–986.
[12] K. Egami, T. Murohara, T. Shimada, K. Sasaki, S. Shintani, T. Sugaya, et al., Role of host angiotensin II type 1 receptor in tumor angiogenesis and growth, J. Clin. Investig. 112 (2003) 67–75.
[13] L. Hu, X.W. Cheng, H. Song, A. Inoue, H. Jiang, X. Li, et al., Cathepsin K activity controls injury-related vascular repair in mice, Hypertension 63 (2014) 607–615.
[14] X.W. Cheng, G.P. Shi, M. Kuzuya, T. Sasaki, K. Okumura, T. Murohara, Role for cysteine protease cathepsins in heart disease focus on biology and mechanisms with clinical implication, Circulation 125 (2012) 1551–1562.
[15] H. Jiang, X.W. Cheng, G.P. Shi, L. Hu, A. Inoue, Y. Yamamura, et al., Cathepsin K-mediated notch1 activation contributes to neovascularization in response to hypoxia, Nat. Commun. 5 (2014) 3838.
[16] G.P. Shi, G.K. Sukhova, M. Kuzuya, Q. Ye, J. Du, Y. Zhang, et al., Deficiency of the cysteine protease cathepsin s impairs microvessel growth, Circ. Res. 92 (2003) 493–500.
[17] B. Wang, J.S. Sun, S. Kitamoto, M. Yang, A. Grubb, H.A. Chapman, et al., Cathepsin s controls angiogenesis and tumor growth via matrix-derived angiogenic factors, J. Biol. Chem. 281 (2006) 6020–6029.
[18] M. Kuzuya, K. Nakamura, T. Sasaki, X.W. Cheng, S. Itohara, A. Iguchi, Effect of MMP-2 deficiency on atherosclerotic lesion formation in apoE-deficient mice, Arterioscler. Thromb. Vasc. Biol. 26 (2006) 1120–1125.
[19] M. Matsumoto, M. Sata, D. Fukuda, K. Tanaka, M. Soma, Y. Hirata, R. Nagai, Orally administered eicosapentaenoic acid reduces and stabilizes atherosclerotic lesions in apoE-deficient mice, Atherosclerosis 197 (2008) 524–533.
[20] X.W. Cheng, M. Kuzuya, W. Kim, H.Z. Song, L.N. Hu, A. Inoue, et al., Exercise training stimulates ischemia-induced neovascularization via phosphatidylinositol 3-kinase/Akt-dependent hypoxia-induced factor-1 alpha reactivation in mice of advanced age, Circulation 122 (2010) 707–716.
[21] X.W. Cheng, M. Kuzuya, K. Nakamura, K. Maeda, M. Tsuzuki, W. Kim, et al., Mechanisms underlying the impairment of ischemia-induced neovascularization in matrix metalloproteinase 2-deficient mice, Circ. Res. 100 (2007) 904–913.
[22] G.K. Sukhova, Y. Zhang, J.H. Pan, Y. Wada, T. Yamamoto, M. Naito, et al., Deficiency of cathepsin s reduces atherosclerosis in LDL receptor-deficient mice, J. Clin. Investig. 111 (2003) 897–906.
[23] T. Sasaki, M. Kuzuya, K. Nakamura, X.W. Cheng, T. Hayashi, H.Z. Song, et al., At1 blockade attenuates atherosclerotic plaque destabilization accompanied by the suppression of cathepsin s activity in apoE-deficient mice, Atherosclerosis 210 (2010) 430–437.
[24] Y.Y. Ji, J.T. Liu, Z.D. Wang, N. Liu, Angiotensin II induces inflammatory response partly via toll-like receptor 4-dependent signaling pathway in vascular smooth muscle cells, Cell Physiol. Biochem. 23 (2009) 265–276.
[25] K.O. Ahn, S.W. Lim, C. Li, H.J. Yang, J.Y. Ghee, J.Y. Kim, et al., Influence of angiotensin II on expression of toll-like receptor 2 and maturation of dendritic cells in chronic cyclosporine nephropathy, Transplantation 83 (2007) 938–947.
[26] G. Trinchieri, A. Sher, Cooperation of toll-like receptor signals in innate immune defence, Nat. Rev. Immunol. 7 (2007) 179–190.
[27] C. Monaco, S.M. Gregan, T.J. Navin, B.M.J. Foxwell, A.H. Davies, M. Feldmann, Toll-like receptor-2 mediates inflammation and matrix degradation in human atherosclerosis, Circulation 120 (2009) 2462–2469.
[28] K.J. Rodgers, D.J. Watkins, A.L. Miller, P.Y. Chan, S. Karanam, W.H. Brissette, et al., Destabilizing role of cathepsin s in murine atherosclerotic plaques, Arterioscler. Thromb. Vasc. Biol. 26 (2006) 851–856.
[29] P.R. Moreno, R. Purushothaman, V. Fuster, D. Echeverri, H. Truszczynska, S.K. Sharma, et al., Plaque neovascularization is increased in ruptured atherosclerotic lesions of human aorta – implications for plaque vulnerability, Circulation 110 (2004) 2032–2038.
[30] Y. Sun, M. Ishibashi, T. Seimon, M. Lee, S.M. Sharma, K.A. Fitzgerald, et al., Free cholesterol accumulation in macrophage membranes activates toll-like receptors and p38 mitogen-activated protein kinase and induces cathepsin K, Circ. Res. 104 (2009), 455–U475.